Critical fields and spontaneous vortex state in the weak-ferromagnetic superconductor RuSr₂GdCu₂O₈

C. Y. Yang, B. C. Chang, and H. C. Ku*
Department of Physics, National Tsing Hua University, Hsinchu, Taiwan 300, R.O.C.

Y. Y. Hsu

Institute of Physics, Academia Sinica, Taipei, Taiwan 115, R.O.C. (Dated: October 28, 2018)

A spontaneous vortex state (SVS) between 30 K and 56 K was observed for the weak-ferromagnetic superconductor RuSr₂GdCu₂O₈ with ferromagnetic Curie temperature T_C = 131 K and superconducting transition temperature T_c = 56 K. The low field (±20 G) superconducting hysteresis loop indicates a narrow Meissner state region within average lower critical field B_{c1}(T)= B_{c1}(0)[1 - (T/T₀)²], with average B_{c1}^{ave}(0) = 12 G and T₀ = 30 K. Full Meissner shielding signal in very low applied field indicates an ab-plane B_{c1}^{ab}(0) ~ 4 G with an estimated anisotropic parameter $\gamma \sim 7$ for this layered system. The existence of a spontaneous vortex state between 30 K and 56 K is the result of weak-ferromagnetic order with a net spontaneous magnetic moment of ~ 0.1 μ_B /Ru, which generates a weak magnetic dipole field around 10 G in the CuO₂ bi-layers. The upper critical field B_{c2} varies linearly as (1 - T/T_c) up to 7-T field. The vortex melting line B_m varies as (1 - T/T_m)^{3.5} with melting transition temperature T_m = 39 K and a very broad vortex liquid region due to the coexistence and the interplay between superconductivity and weak-ferromagnetic order.

PACS numbers: 74.72.-h, 74.25.Ha

I. INTRODUCTION

Recently, high-T_c superconductivity with anomalous magnetic properties was reported in the weak-ferromagnetic Ru-1212 system RuSr₂RCu₂O₈ (R = Sm, Eu, Gd, Y) with the tetragonal TlBa₂CaCu₂O₇-type structure. 1,2,3,4,5,6,7,8,9,10,11,12,13,14,15,16,17,18,19,20,21,22,23,24,25

For the Ca-substituted system, a possible superconductivity was also reported in the weak-ferromagnetic compounds $RuCa_2RCu_2O_8$ (R = Pr-Gd). 44,45,46 The metallic weak-ferromagnetic (WFM) order is originated from the long range order of Ru moments in the RuO_6 octahedra due to strong Ru-4
d $_{xy,yz,zx}$ -O-2 $\mathrm{p}_{x,y,z}$ hybridization in this strongly-correlated electron system. The Curie temperature $T_C \sim 130$ K observed from magnetization measurement in the prototype compound RuSr₂GdCu₂O₈ is probably a canted G-type antiferromagnetic order with Ru⁵⁺ moment μ canted along the tetragonal basal plane resulting a small net spontaneous magnetic moment $\mu_s \ll \mu(Ru^{5+})$ too small to be detected in neutron diffraction. 4,5,9,10,21 The occurrence of high- T_c superconductivity with maximum resistivity onset $T_c(\text{onset}) \sim 60 \text{ K in } \text{RuSr}_2\text{GdCu}_2\text{O}_8$ is related with the quasi-two-dimensional CuO_2 bilayers separated by a rare earth layer in the Ru-1212 structure. 1,2,4,5,29 Broad resistivity transition width $\Delta T_c = T_c(\text{onset}) - T_c(\text{zero}) \sim 15\text{-}20 \text{ K observed is most}$ likely originated from the coexistence and the interplay between superconductivity and weak-ferromagnetic order. 1,2,3,4,5,6,7,8,9,10,11,12,13,14,15,16,17,18,19,20,21,22,23,24,25,26,2

The diamagnetic T_c is observed anomalously at lower temperature near $T_c(\text{zero})$ instead of at $T_c(\text{onset})$, and a reasonable large Meissner signal was reported using stationary sample magnetometer with diamagnetic

 $T_c \sim 30 \text{ K in} \leq 1 \text{ G applied field at zero-field-cooled (ZFC) mode.}^{38} \text{ Lower } T_c(\text{onset}) \sim 40 \text{ K and } 12 \text{ K}$ were observed for RuSr₂EuCu₂O₈ and RuSr₂SmCu₂O₈, respectively.^{12,17} No superconductivity can be detected in RuSr₂RCu₂O₈ (R = Pr, Nd).^{3,16} Superconducting RuSr₂YCu₂O₈ phase is stable only under the high pressure.^{20,25}

pressure 20,25

II. EXPERIMENTAL

The stoichiometric RuSr₂GdCu₂O₈ samples were synthesized by the standard solid-state reaction method. High-purity RuO₂ (99.99 %), SrCO₃ (99.99 %), Gd₂O₃ (99.99 %), and CuO (99.99 %) preheated powders with the nominal composition ratio of Ru:Sr:Gd:Cu = 1: 2: 1: 2 were well mixed and calcined at 960°C in air for 16 hours. The calcined powders were then pressed into pellets and sintered in flowing N₂ gas at 1015°C for 10 hours to form RuSr₂GdO₆ and Cu₂O precursors. This step is crucial in order to avoid the formation of unwanted impurity phases. The N₂-sintered pellets were heated at 1060°C in flowing O₂ gas for 10 hours to form the Ru-7222-phase²-3The perfects were 40xygen²-annealed at slightly higher 1065°C for 5 days and slowly furnace-cooled to room temperature with a rate of 15°C per hour.¹⁵

The powder x-ray diffraction data were collected with a Rigaku Rotaflex 18-kW rotating anode diffractometer

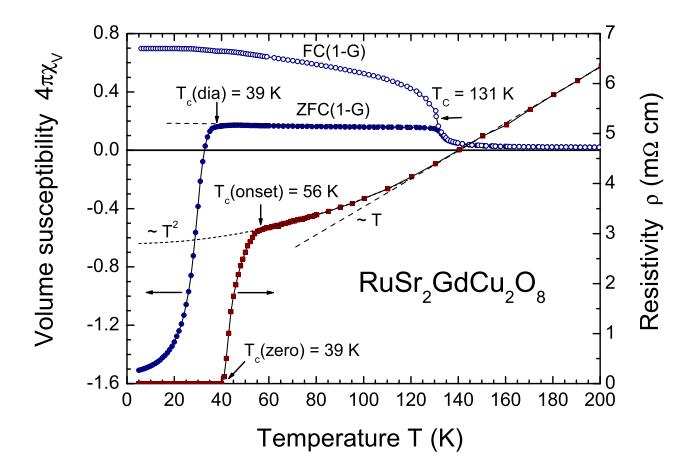


FIG. 1: Electrical resistivity $\rho(T)$ and volume magnetic susceptibility $\chi_V(T)$ at 1-G field-cooled (FC) and zero-field-cooled (ZFC) modes for oxygen-annealed RuSr₂GdCu₂O₈

using graphite monochromatized Cu-K $_{\alpha}$ radiation with a scanning step of 0.02° (10 second counting time per step) in the 2 θ ranges of 5-100°. The electrical resistivity and magneto-resistivity measurements were performed using the standard four-probe method with a Linear Research LR-700 ac (16Hz) resistance bridge from 2 K to 300 K with applied magnetic field up to 7 T. The magnetization, magnetic susceptibility and magnetic hysteresis measurements from 2 K to 300 K with applied fields from 1 G to 7 T were carried out with a Quantum Design 1-T μ -metal shielded MPMS2 or a 7-T MPMS superconducting quantum interference device (SQUID) magnetometer.

III. RESULTS AND DISCUSSION

The powder x-ray diffraction pattern for the oxygenannealed RuSr₂GdCu₂O₈ polycrystalline sample indicates close to single phase with the tetragonal lattice parameters of a=0.5428(5) nm and c=1.1589(9) nm. The space group P4/mbm is used for Rietveld refinement analysis, where neutron diffraction data indicate that a RuO₆ octahedra 14° rotation around the c-axis is needed to accommodate physically reasonable Ru-O bond lengths.¹⁰ The refinement gives a good residual error R of 3.64 %, weighted pattern error $R_{wp}=6.07$ %, and Bragg error $R_B=5.05$ %.

The temperature dependence of the electrical resistivity $\rho(T)$ and the volume magnetic susceptibility $\chi_V(T)$ at 1-G field-cooled (FC) and zero-field-cooled (ZFC) modes for RuSr₂GdCu₂O₈ are shown collectively in Fig. 1. The high temperature resistivity decreases monotonically from room temperature value of 9.2 m Ω .cm (not shown) to 6.4 m Ω .cm at 200 K, and extrapolated to 2.8 m Ω .cm at 0 K with a good resistivity ratio $\rho(300 \text{ K})/\rho(0 \text{ K})$ of 3.3 for the polycrystalline sample. High temperature resistivity shows a non-Fermi-liquid-like linear T-dependence down to Curie temperature T_C of 131 K, then changes

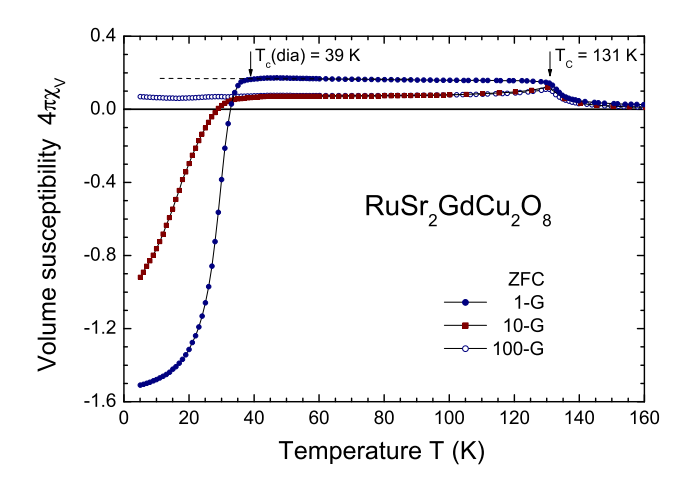


FIG. 2: ZFC volume susceptibility $\chi_V(T)$ for RuSr₂GdCu₂ O₈ at 1 G, 10 G, and 100 G. Note that the full Meissner shielding signal was observed only at low applied field and low temperature.

to a T^2 behavior below T_C due to magnetic order.

The superconducting onset temperature of 56 K is determined from the deviation from T² behavior, with a zero resistivity $T_c(zero)$ at 39 K. The broad transition width $\Delta T_c = 17$ K observed is the common feature for all reported Ru-1212 resistivity data, which indicates that the superconducting Josephson coupling along the tetragonal c-axis between Cu-O bi-layers may be partially blocked by the dipole field B_{dipole} of ordered Ru moments in the Ru-O layer. 1,2,4,5,29,40 The diamagnetic T_c at 39 K was observed in the 1-G ZFC susceptibility measurement. The full Meissner shielding signal $4\pi\chi_V$ $= 4\pi M/B_a \sim -1.5$ (Gaussian units) was recorded at 5 K. This value is identical to the Meissner shielding signal expected for a superconducting sphere with a demagnetization factor N of $-4\pi/3$ and in an applied field B_a well below lower critical field B_{c1} . The large diamagnetic signal in 1-G ZFC mode is the best data observed so far from various reported susceptibility measurement techniques. 4,5,28,29,38 Since our measurements were performed with the standard moving-sample SQUID magnetometer, it is clear that sample quality is more crucial than measuring techniques. Both ZFC and FC data reveal a Curie temperature T_C of 131 K. However, in 1-G FC mode, no diamagnetic field-expulsion signal can be detected below 39 K due to strong flux pinning where superconductivity coexists with weak-ferromagnetic order.

The zero-field-cooled (ZFC) volume susceptibility $\chi_V({\rm T})$ at 1 G, 10 G, and 100 G applied fields are shown collectively in Fig. 2. All data show the same magnetic order ${\rm T}_C({\rm Ru})$ of 131 K. Although the diamagnetic ${\rm T}_c$ of 39 K was still observed at 10-G ZFC measurement, the diamagnetic signal at 5 K is reduced to 60% of the full Meissner signal. Consider the polycrystalline nature of sample with varying microcrystallite size and orientation, the average superconducting lower critical field ${\rm B}_{c1}$ at 5

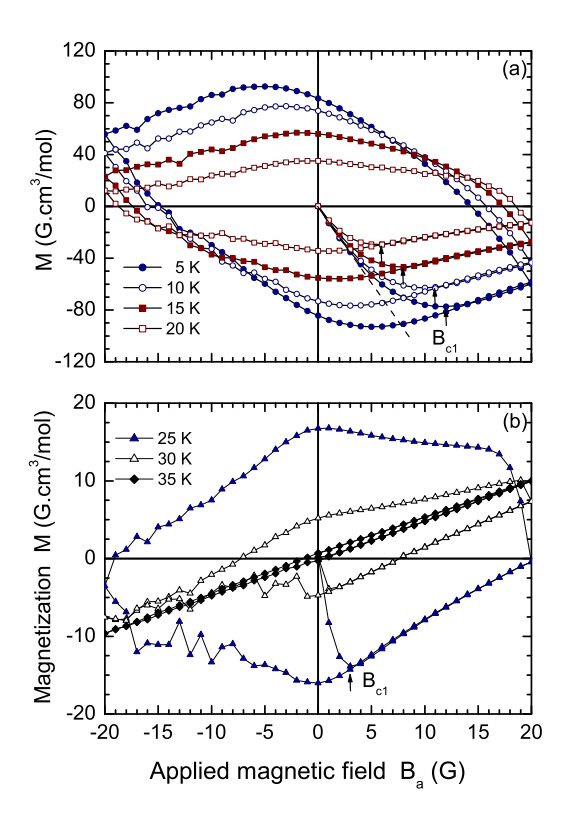


FIG. 3: Low field superconducting hysteresis loops M-B_a for RuSr₂GdCu₂O₈: (a) at 5 K, 10 K, 15 K, 20 K; (b) at 25 K, 30 K, and 35 K.

K is estimated to be close to 10 G. No net diamagnetic signal can be detected at 100-G ZFC mode where the sample is already in the vortex glass or lattice state and the small diamagnetic signal is overshadowed by a large weak-ferromagnetic background.³⁸

Based on this information, the low-field (± 20 G) isothermal superconducting hysteresis loops $M-B_a$ are measured and collectively shown in Fig. 3(a) (5 K, 10 K, 15 K, and 20 K) and 3(b) (25 K, 30 K, and 35 K). The initial magnetization curve deviates from straight line in 4 G at 5 K, 3.5 G at 10 K, 3 G at 15 K, 2 G at 20 K, and 1 G at 25 K. This is the narrow region that full Meissner signals are detected and is roughly corresponding to the anisotropic lower critical field in the ab-plane $B_{c1}^{ab}(T)$ with $B_{c1}^{ab}(0) \sim 4$ G. The average lower critical field B_{c1}^{ave} for polycrystalline sample is determined from the peaks of initial diamagnetic magnetization curves. B_{c1} decreases steadily from 12 G at 5 K, 11 G at 10 K, 9 G at 15 K, 6 G at 20 K, 3 G at 25 K and below 1 G at 30 K. A simple empirical parabolic fitting gives $B_{c1}(T) = B_{c1}(0)[1$ - $(T/T_0)^2$], with average $B_{c1}^{ave}(0) = 12$ G and $T_0 = 30$ K (see Fig. 4). Using the anisotropic Ginzburg-Landau formula $B_{c1}^{ave}=[2B_{c1}^{ab}+B_{c1}^{c}]/3$, c-axis $B_{c1}^{c}\sim28$ G and anisotropy parameter $\gamma \sim 7$ is estimated. This value is close to reported anisotropic γ-value for YBa₂Cu₃O₇ where the 123-type structure can be written as Cu-1212 $CuBa_2YCu_2O_7$. An average penetration depth $\lambda_{ave}(0)$ $= [\Phi_0/2\pi B_{c1}^{ave}(0)]^{1/2} \text{ of 520 nm was derived with esti-}$

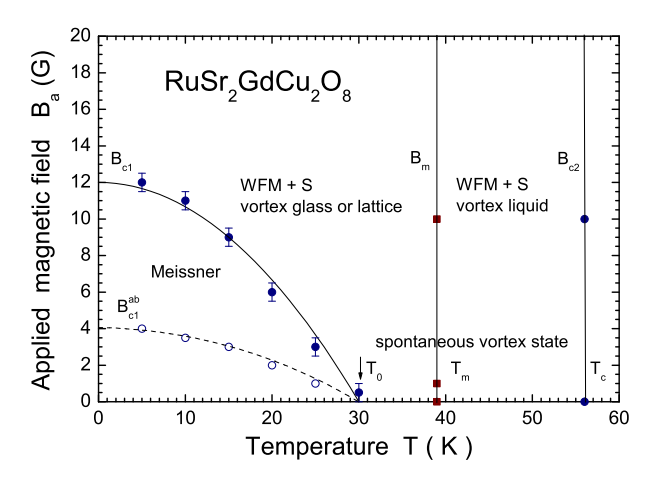


FIG. 4: The lower field, low temperature superconducting phase diagram $B_a(T)$ of RuSr₂GdCu₂O₈.

mated $\lambda_{ab}(0)=340$ nm and $\lambda_c(0)=2400$ nm from $\mathbf{B}_{c1}^c=\Phi_0/2\pi\lambda_{ab}^2$ and $\mathbf{B}_{c1}^{ab}=\Phi_0/2\pi\lambda_{ab}\lambda_c$, where Φ_0 is flux quantum.

Since $T_0 = 30 \text{ K}$ is well below $T_c(\text{onset}) = 56 \text{ K}$ and $T_c(zero) = 39 \text{ K in zero applied field, a spontaneous vor-}$ tex state (SVS) indeed exists between 30 K and 56 K. The low field phase diagram $B_a(T)$ for polycrystalline sample is shown in Fig. 4, with the average $B_{c1}(T)$ separates the Meissner state from the vortex state and a smaller $B_{c1}^{ab}(T)$ inside the Meissner region for reference. $T_c(zero) = 39 \text{ K}$ in the broad resistive transition is the onset of vortex depinning by driving current. This temperature is very close to the melting transition temperature T_m from the spontaneous vortex glass or lattice state to the spontaneous liquid state due to nonzero dipole field B_{dipole} of weak-ferromagnetic order. The upper critical field B_{c2} defined from T_c (onset) and the vortex melting field $B_m(T)$ defined from $T_c(zero)$ are temperature independent for small applied fields below 20 G. The internal dipole field generated by a weak-ferromagnetic order can be estimated using a simple extrapolation $[B_{c1}(0)+$ $B_{dip}/B_{c1}(0) = T_c/T_0 = 56 \text{ K/30 K}$, which results with a dipole field $B_{dipole} \sim 10.4$ G on the CuO_2 bi-layers. A small net spontaneous magnetic moment μ_s of ~ 0.11 μ_B per Ru is estimated using $B_{dipole} \sim 2\mu_s/d^3$ with d = c/2 = 0.58 nm is the distance between midpoint of CuO₂ bi-layers and two nearest-neighbor Ru moments. If the weak-ferromagnetic structure is a canted G-type antiferromagnetic order with Ru moments μ (= 1.5 μ_B for Ru^{5+} in t_{2q} states) canted along the tetragonal basal plane, the small net spontaneous magnetic moment gives a canting angle of 4° from the tetragonal c-axis and is difficult to be detected in neutron diffraction with a resolution around 0.1 μ_B . 9,10,21

At 5 K, the shape of superconducting hysteresis loop with a large remanent molar magnetization M_r of 83 $G.cm^3/mol$ indicates strong pinning as well as a good indication of bulk nature of superconductivity for the oxygen-annealed sample. The remanent M_r decreases

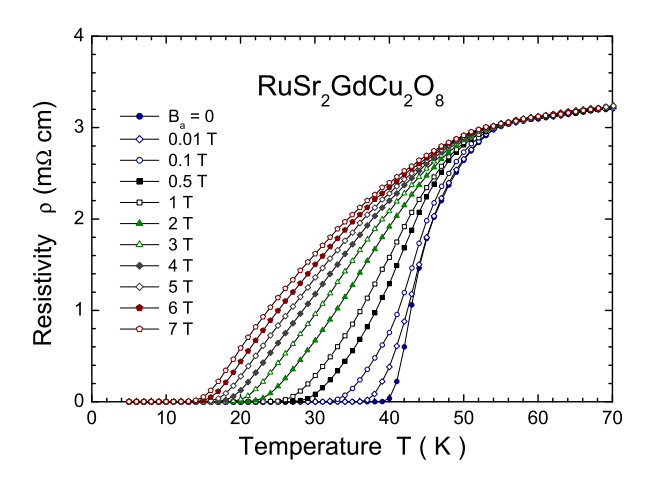


FIG. 5: Temperature dependence of magnetoresistivity $\rho(T, B_a)$ for RuSr₂GdCu₂O₈ in applied field up to 7 T.

to 4 G.cm³/mol at 30 K and 1 G.cm³/mol at 35 K, where a weak-ferromagnetic background can be clearly seen. Fluctuation in the hysteresis loop is probably also related to the weak-ferromagnetic order.

To study the high-field effect on superconductivity, the magnetoresistivity $\rho(T,B_a)$ for RuSr₂GdCu₂O₈ up to 7 T are collectively shown in Fig. 5. The broadening of resistive transition in magnetic fields is the common features for all high- T_c cuprate superconductors.⁴⁷ The normal state resistivity is field independent and follows a T^2 dependence below T_C , with superconducting T_c (onset) of 56 K in zero field decreases slightly to 53 K in 7-T field. The temperature dependence of upper critical field $B_{c2}(T)$ can be fitted with a linear function $B_{c2}(0)[1 T/T_c$] with average $B_{c2}(0) = 133 \text{ T.}^{47}$ An average coherence length $\xi_0^{ave} = [\Phi_0/2\pi B_{c2}^{ave}(0)]^{1/2}$ of 0.5 nm with the Ginzburg-Landau parameter κ of 1040 and the thermodynamic critical field $B_c(0) = (B_{c1}.B_{c2})^{1/2} = 0.32 \text{ T}.$ No anisotropic ξ_{ab} and ξ_c values can be estimated from present data. The $T_c(zero)$ decreases from 39 K in zero applied field to 32 K in 1-kG, 28 K in 5-kG, 25 K in 1-T, 22 K in 2-T, 19 K in 3-T, 17 K in 4-T, 16 K in 5-T, 15 K in 6-T, and 14 K in 7-T field. If the zero resistivity is taken as the lower bound of the vortex melting temperature T_m , then the temperature dependence of the vortex melting transition line $B_m(T)$ can be fitted roughly by the formula $B_m(T) = B_m(0)[1 - T/T_m]^{3.5}$ with $B_m(0) =$ 35 T and large exponent 3.5. In the lower field region, $B_m(T)$ rises as $[1 - T/T_m]^2$ as predicted by the mean-field approximation for temperature near $T_m = 39 \text{ K.}^{47}$ The full phase diagram $B_a(T)$ of $RuSr_2GdCu_2O_8$ is shown in Fig. 6 to exhibit both high field and low field features. The very broad vortex liquid region with $\Delta T = 17 \text{ K}$ in zero field and $\Delta T = 42$ K in 7-T field is extraordinary and is most likely originated from the coexistence and the interplay between superconductivity and weakferromagnetic order. This magnetic order is so weak that superconductivity can coexist with the magnetic order, but the effect of a weak spontaneous magnetic moment

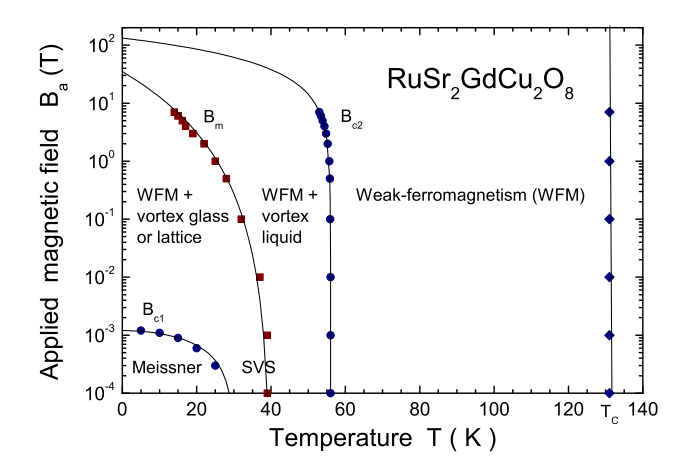


FIG. 6: Full phase diagram $B_a(T)$ of $RuSr_2GdCu_2O_8$.

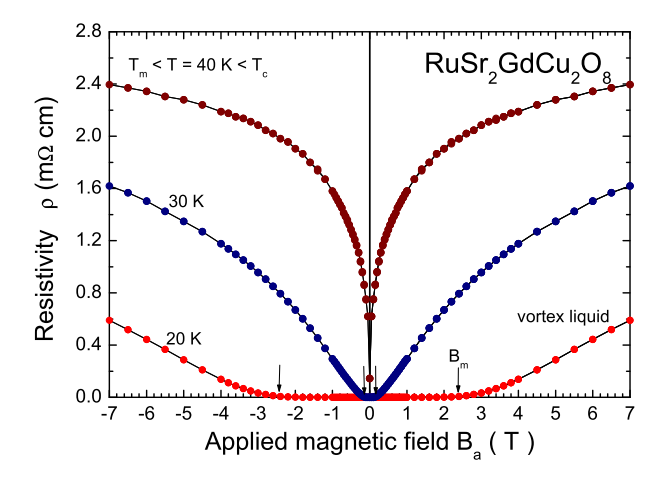


FIG. 7: Field dependence of magnetoresistivity $\rho(B_a)$ for RuSr₂GdCu₂O₈ in the vortex state at 20 K, 30 K, and 40 K.

 $\mu_s \sim 0.1~\mu_B$ is detected through the appearance of a spontaneous vortex state above 30 K with a broad spontaneous vortex liquid region above T_m of 39 K.

To study the broad vortex liquid region, the isothermal field-dependent magnetoresistivity $\rho(B_a)$ for $T < T_c$ are shown in Fig. 7, where zero resistivity gives a lower bound of vortex melting field B_m . In the resistive vortex liquid region, there is no unique power-law fit, but the data can be roughly fitted with various powers between 1/6 and 1, depending on temperature range. At T=40 K $> T_m=39$ K, resistivity is $\sim B_a^{1/6}$ for $B_a>2$ T and gradually changes to $\sim B_a^{1/3}$ below 1 T. At 30 K with $B_m=0.2$ T, resistivity $\sim B_a^{2/3}$ for $B_a>2$ T and gradually changes to linear B_a below 1 T. At 20 K with $B_m\sim2.4$ T, similar linear variation of resistivity with B_a was observed for $B_a>3.5$ T.

The last issue to be addressed is the depression of T_c by small spontaneous Ru magnetic moments. The weak-ferromagnetic order is actually a canted antiferromagnetic order that can coexist with superconductivity. However, the observed T_c of 56 K is too low as compared

with 93 K for YBa₂Cu₃O₇ or 103 K for TlBa₂CaCu₂O₇. The depression of T_c by small spontaneous magnetic moment can be partially recovered by substitution of nonmagnetic Cu ions at Ru site. For example, in the Ru_{1-x}Cu_xSr₂GdCu₂O₈ system, T_c onset up to 65 K for x = 0.1 and 72 K for x = 0.4 was reported. 26,29

IV. CONCLUSION

The lower critical field with $B_{c1}(0) = 12$ G and $T_0 = 30$ K indicates the existence of a spontaneous vortex state (SVS) between 30 K and T_c of 56 K. This SVS state is closely related with the weak-ferromagnetic order

with a net spontaneous magnetic moment of $\sim 0.1~\mu_B$ per Ru. The broad vortex liquid region observed above vortex melting line $B_m(T)$ is also due to the coexistence and the interplay between superconductivity and weak-ferromagnetic order.

Acknowledgments

This work was supported by the National Science Council of R.O.C. under contract No. NSC93-2112-M007-011. We thank Dr. B. N. Lin for helpful discussions.

- * Electronic address: hcku@phys.nthu.edu.tw
- ¹ L. Bauernfeind, W. Widder, and H. F. Braun, Physica C 254, 151 (1995).
- ² L. Bauernfeind, W. Widder, H. F. Braun, J. Low Temp. Phys. **105**, 1605 (1996).
- ³ K. B. Tang, Y. T. Qian, L. Yang, Y. D. Zhao, Y. H. Zhang, Physica C 282-287, 947 (1997).
- ⁴ J. L. Tallon, C. Bernhard, M. Bowden, P. Gilberd, T. Stoto, and D. Pringle, IEEE Trans. Appl. Supercon. 9, 1696 (1999).
- ⁵ C. Bernhard, J. L. Tallon, Ch. Niedermayer, Th. Blasius, A. Golnik, E. Brucher, R. K. Kremer, D. R. Noakes, C. E. Stronach, and E. J. Ansaldo, Phys. Rev. B **59**, 14099 (1999).
- ⁶ A. C. McLaughlin, W. Zhou, J. P. Attfield, A. N. Fitch, and J. L. Tallon, Phys. Rev. B **60**, 7512 (1999).
- J. L. Tallon, J. W. Loram, G. V. M. Williams, and C. Bernhard, Phys. Rev. B 61, R6471 (2000).
- ⁸ C. Bernhard, J. L. Tallon, E. Brucher, and R. K. Kremer, Phys. Rev. B **61**, R14960 (2000).
- ⁹ J. W. Lynn, B. Keimer, C. Ulrich, C. Bernhard, and J. L. Tallon, Phys. Rev. B **61**, R14964 (2000).
- O. Chmaissem, J. D. Jorgensen, H. Shaked, P. Dollar, and J. L. Tallon, Phys. Rev. B **61**, 6401 (2000).
- ¹¹ G. V. M. Williams, and S. Kramer, Phys. Rev. B **62**, 4132 (2000).
- ¹² C. W. Chu, Y. Y. Xue, S. Tsui, J. Cmaidalka, A. K. Heilman, B. Lorenz, and R. L. Meng, Physica C **335**, 231 (2000).
- ¹³ A. C. Mclaughlin, V. Janowitz, J. A. McAllister, and J. P. Attfield, Chem. Commun. 2000, 1331 (2000).
- ¹⁴ X. H. Chen, Z. Sun, K. Q. Wang, Y. M. Xiong, H. S. Yang, H. H. Wen, Y. M. Ni, Z. X. Zhao, J. Phys. Cond. Mat. **12**, 10561 (2000).
- ¹⁵ R. L. Meng, B. Lorenz, Y. S. Wang, J. Cmaidalka, Y. Y. Xue, and C. W. Chu, Physica C **353**, 195 (2001).
- ¹⁶ V. P. S. Awana, J. Nakamura, M. Karppinen, H. Yamauchi, S. K. Malik, and W. B. Yelon, Physica C **357-360**, 121 (2001).
- ¹⁷ D. P. Hai, S. Kamisawa, I. Kakeya, M. Furuyama, T. Mochiku, and K. Kadowaki, Physica C **357-360**, 406 (2001).
- ¹⁸ Å. P. Litvinchuk, S. Y. Chen, M. N. Ilive, C. L. Chen, C. W. Chu, and V. N. Popov, Physica C **361**, 234 (2001).

- ¹⁹ C. T. Lin, B. Liang, C. Ulrich, C. Berhard, Physica C **364-365**, 373 (2001).
- ²⁰ H. Takagiwa, J. Akimitsu, H. Kawano-Furukawa, and H. Yoshizawa, J. Phys. Soc. Jpn. **70**, 333 (2001).
- ²¹ J. D. Jorgensen, O. Chmaissem, H. Shaked, S. Short, P. W. Klamut, B. Dabrowski, and J. L. Tallon, Phys. Rev. B 63, 054440 (2001).
- ²² R. S. Liu, L.-Y. Jang, H.-H Hung, and J. L. Tallon, Phys. Rev. B **63**, 212507 (2001).
- ²³ M. Pozek, A. Dulcic, P. Paar, G. V. M. Williams, and S. Kramer, Phys. Rev. B **64**, 064508 (2001).
- ²⁴ V. G. Hadjiew, J. Backstrom, V. N. Popov, M. N. Iliev, R. L. Meng, Y. Y. Xue, and C. W. Chu, Phys. Rev. B **64**, 134304 (2001).
- Y. Tokunaga and H. Kotegawa and K. Ishida and Y. Kitaka and H. Takagiwa and J. Akimitsu, Phys. Rev. Lett. 86, 5767 (2001).
- ²⁶ P. W. Klamu, B. Dabrowski, S. Kolesnik, M. Maxwell, and J. Mais, Phys. Rev. B **63**, 224512 (2001).
- ²⁷ B. Lorenz, Y. Y. Xue, R. L. Meng, and C. W. Chu, Phys. Rev. B **65**, 174503 (2002).
- ²⁸ T. P. Papageorgiou, H. F. Braun, and T. Herrmannsdorfer, Phys. Rev. B 66, 104509 (2002).
- ²⁹ H. Fujishiro, M. Ikebe, and T. Takahashi, J. Low Temp. Phys. **131**, 589 (2003).
- ³⁰ C. Shaou, H. F. Braun, and T. P. Papageorgiou, J. Alloys and Compounds 351, 7 (2003).
- ³¹ A. Vecchione, M. Gombos, C. Tedesco, A. Immirzi, L. Marchese, A. Frache, C. Noce, and S. Pace, Intern. J. Mod. Phys. B 17, 899 (2003).
- ³² F. Cordero, M. Ferretti, M. R. Cimberle, and R. Masini, Phys. Rev. B **67**, 144519 (2003).
- ³³ H. Sakai, N. Osawa, K. Yoshimura, M. Fang, and K. Kosuge, Phys. Rev. B 67, 184409 (2003).
- ³⁴ Y. Y. Xue, F. Chen, J. Cmaidalka, R. L. Meng, and C. W. Chu, Phys. Rev. B **67**, 224511 (2003).
- ³⁵ J. E. McCrone, J. L. Tallon, J. R. Cooper, A. C. MacLaughlin, J. P. Attfield, and C. Bernhard, Phys. Rev. B 68, 064514 (2003).
- ³⁶ A. Lopez, I. S. Azevedo, J. E. Musa, and E. Baggio-Saitovitch, Phys. Rev. B 68, 134516 (2003).
- ³⁷ S. Garcia, J. E. Musa, R. S. Freitas, and L. Ghivelder, Phys. Rev. B **68**, 144512 (2003).
- ³⁸ T. P. Papageorgiou, H. F. Braun, T. Gorlach, M. Uhlarz,

- and H. v. Lohneysen, Phys. Rev. B 68, 144518 (2003).
- ³⁹ P. W. Klamut, B. Dabrowski, S. M. Mini, M. Maxwell, J. Mais, I. Felner, U. Asaf, F. Ritter, A. Shengelaya, R. Khasanov, I. M. Savic, H. Keller, A. Wisniewski, R. Puzniak, I. M. Fita, C. Sulkowski, and M. Matusiak, Physica C 387, 33 (2003).
- ⁴⁰ T. Nachtrab, D. Koelle, R. Kleiner, C. Bernhard, and C. T. Lin, Phys. Rev. Lett. **92**, 117001 (2004).
- ⁴¹ Y. Y. Xue and B. Lorenz and A. Baikalov and J. Cmaidaka and F. Chen and R. L. Meng and C. W. Chu, Physica C 408-410, 638 (2004).
- ⁴² S. Garcia and L. Ghivelder, Phys. Rev. B **70**, 052503 (2004).
- 43 C. J. Liu., C. S. Sheu, T. W. Wu, L. C. Huang, F. H. Hsu,

- H. D. Yang, G. V. M. Williams, and C. C. Liu, Phys. Rev. B 71, 014502 (2004).
- ⁴⁴ Y. C. Lin and T. Y. Chiu and M. F. Tai and B. N. Lin and P. C. Guan and H. C. Ku, Intern. J. Mod. Phys. B **19**, 339 (2005).
- ⁴⁵ T. Y. Chiu and Y. C. Lin and M. F. Tai and B. N. Lin and P. C. Guan and B. C. Chang and H. C. Ku, Chin. J. Phys. 43, 616 (2005).
- ⁴⁶ H. C. Ku and C. Y. Yang and B. C. Chang and B. N. Lin and Y. Y. Hsu and M. F. Tai, J. Appl. Phys. **97**, 10B110 (2005).
- ⁴⁷ M. Tinkham, Introduction to Superconductivity (McGraw-Hill, Inc. Singapore, 1996), ch. 9.